Power Fluctuations From Large Wind Farms

Poul Sørensen, *Senior Member, IEEE*, Nicolaos Antonio Cutululis, *Member, IEEE*, Antonio Vigueras-Rodríguez, Leo E. Jensen, Jesper Hjerrild, Martin Heyman Donovan, and Henrik Madsen

***Abstract*—This paper deals with power fluctuations from wind farms. The time range in focus is between one minute and up to a couple of hours. In this time range, substantial power fluctuations have been observed during unstable weather conditions. A wind power fluctuation model is described, and measured time series from the first large offshore wind farm, Horns Rev in Denmark, are compared to simulated time series. The comparison between measured and simulated time series focuses on the ramping characteristics of the wind farm at different power levels and on the need for system generation reserves due to the fluctuations. The comparison shows a reasonable agreement between simulations and measurements, although there is still room for improvement of the simulation model.**

***Index Terms*—Frequency control, power control, spectral analysis, wind power generation.**

I. Introduction

A fundamental issue in the operation and control of electric power systems is to maintain the balance between generated and demanded power. Scheduling of generation ensures that sufficient generation power is available to follow the forecasted load, hour by hour during the day [1]. Besides, sufficient reserves with response times from seconds to minutes must be available to balance the inevitable deviations from the schedules caused by failures and forecast errors.

In the Nordic power system, the generation is scheduled on the NORDPOOL spot market [2] on the day-ahead spot market, while the reserve capacities are agreed in the Nordel cooperation between the Nordic transmission system operators [3]. Those reserves include a "fast active disturbance reserve," which is regulating power that must be available 15 min after allocation. The purpose of the regulating power is to restore the frequency controlled reserves, which are activated due to frequency deviations from the nominal value. The frequency controlled reserves are much faster than the regulating power, with required response times from a few minutes down to a few seconds, depending on the frequency error.

The wind power development influences the power balancing on all time scales. Wind power forecasts have been studied already when there was much less wind power in the systems than today, e.g., Troen and Landberg [4]. The wind power forecasts are used by the stakeholders on the day-ahead market to reduce the forecast errors caused by wind variability and thereby optimize the bits on the market. On a shorter time scale, wind power variability also influences the power balancing, although this influence seems to become an issue only with a significantly higher amount of wind power in the system.

An example of this is the experience of the Danish transmission system operator, Energinet.dk, with the operation of the West Danish power system. According to Akhmatov *et al.* [5], Energinet.dk has found that the active power supplied from the first large 160-MW offshore wind farm in this system, Horns Rev, is characterized by more intense fluctuations in the minute range than previously observed form the dispersed wind turbines on land, even though the installed power in Horns Rev is relatively small compared to the total 2400-MW wind power installation in the system.

Fig. 1 shows the power generation in January 18, 2005 of the wind turbines observed by the then owning power producer Elsam. It is divided into the power fluctuations from the Horns Rev wind farm and the fluctuations in the production of the "Onshore" wind turbines with a comparable installed capacity.

The selected day is characterized by very unstable weather conditions, and therefore, the power fluctuations from the Horns Rev wind farm are exceptionally high. At the same time, the fluctuations in the production of the "Onshore" wind turbines are much less.

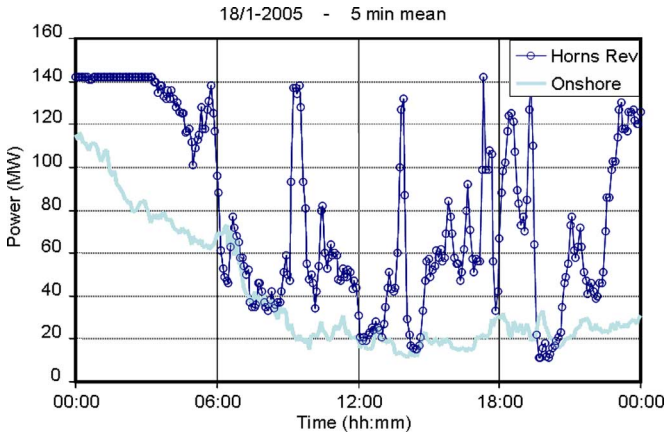

Fig. 1. Power generation of Horns Rev offshore wind farm and onshore wind turbines on January 18, 2005.

Manuscript received September 6, 2006; revised December 11, 2006. This work was supported by the Danish Transmissions System Operator, Energinet.dk, under research program PSO 2004, Grant 6506. Paper no. TPWRS-00603-2006.

P. Sørensen and N. A. Cutululis are with Risø National Laboratory, Roskilde DK-4000, Denmark (e-mail: poul.e.soerensen@risoe.dk; nicolaos.cutululis@risoe.dk).

A. Vigueras-Rodríguez is with Universidad Politécnica de Cartagena, Cartagena, Spain.

L. E. Jensen and J. Hjerrild are with Elsam (now a part of Dong Energy) Engineering, Fredericia DK-7000, Denmark.

M. H. Donovan is with Energi E2, Copenhagen DK-2450, Denmark.

H. Madsen is with the Technical University of Denmark, Lyngby DK-2800, Denmark.

Color versions of one or more of the figures in this paper are available online at http://ieeexplore.ieee.org.

Digital Object Identifier 10.1109/TPWRS.2007.901615

Generally, the onshore wind power fluctuates much less than the Horns Rev wind farm, first of all because the offshore turbines are concentrated in a very small area where the wind speed fluctuations are much more correlated than the wind speeds at the turbines dispersed over a much bigger area. Another reason that may increase the fluctuations from Horns Rev is that the meteorological conditions are different offshore than onshore.

The West Danish power system is dc connected to the Nordic synchronous power system, and it is a part of the Nordel cooperation. At the same time, the system is interconnected to the Central European UCTE system through the German ac connection. Therefore, the West Danish system also has obligations to the UCTE system, including the responsibility to keep the agreed power flow in this interconnection within acceptable limits.

To some extent, these fluctuations can be handled by the Wind Farm Main Controller, using the power rate limiter in that controller [6]. The power rate limiter can only reduce the power, i.e., produce less than what is available according to, e.g., Fig. 1. Therefore, the power rate limiter can efficiently limit the positive ramp rate, while the negative ramp rate is more difficult to limit. Still, also the negative power ramping would be significantly reduced with a limited positive ramp rate, because it would cut the power peaks in Fig. 1.

With the present wind power capacity, the power flow in the interconnection can be kept within the agreed limits. However, a second neighboring wind farm, the 200-MW Horns Rev B, is already scheduled for 2008, and Energinet.dk is concerned how this will influence the future demand for regulating power in the system.

In the United States, several detailed technical investigations of grid ancillary service impacts of wind power plants have been performed recently. Parson *et al.* [7] summarizes the studies, which are also focused on the wind power variability. In the United States, the utilities deal with both load following and regulation on a control area basis, which is similar to the tasks of Energinet.dk in the West Danish control area. The studies in the United States quantify the impact of wind farms on load following as well as regulation power, based on measurements on several large wind farms.

On small island power systems, wind power fluctuations may have even more severe consequences for the operation and security of the system. An example of such a system is the island of Hawaii, which is not interconnected to other systems. The ability to integrate wind power in the system on the island of Hawaii is also limited by the generation resource mix, which includes a relatively large amount of non-regulating generating units [8]. The system operator HELCO has introduced wind power performance standards with limits for the wind power fluctuations in the seconds to minute range.

Wind power fluctuations are also a security issue in systems with very weak interconnections. The island of Ireland is a significant example of such a system, which has only a very weak connection to Scotland. Another example is the Iberian Peninsula with a weak connection to France.

This paper will quantify the power fluctuations measured on the Horns Rev wind farm and compare the measured power fluctuations to simulated power fluctuations. Section II describes the applied simulation model, Section III describes the site and data acquisition on Horns Rev wind farm, and Section IV presents the analyses. Finally, the conclusions are drawn in Section V.

II. Simulation Model

The power fluctuation model is based on the wind speed fluctuation model developed by Sørensen *et al.* [9]. This wind speed model has been applied by Rosas [10] to simulate the wind speed fluctuations from one wind turbine to wind farms with 30, 150, and 300 wind turbines, respectively. The simulated power time series were, however, significantly less fluctuating than typical power time series measured on real wind farms. The main reason for the underestimation of the power fluctuations is that only turbulence on a time scale from seconds to a few minutes was included.

This result has initiated new studies of the characteristics of fluctuating wind speeds, based on measurements on Risø's test site for large wind turbines [11] placed on flat land approximately 2 km from the west coast to the North Sea. The focus has been on the slower variations in wind speeds, including the coherences between wind speeds measured over horizontal distances.

The simulation model uses a statistical description of the wind speed characteristics given in the frequency domain to simulate time series of output power from a wind farm. A detailed description is given in [12]. In this section, a shorter description is provided to support the analyses and conclusions.

The basic structure of the simulation model is shown in Fig. 2. The wind farm consists of N wind turbines, indexed with i between 1 and N.

The inputs to the model is the N power spectral densities (PSDs) $S_{u[i]}(f)$ of wind speeds $u_{[i]}(t)$ in hub height of the wind turbines, and the $N \times N$ coherence functions $\gamma_{[r,c]}(f)$ between $u_{[r]}(t)$ and $u_{[c]}(t)$. The output from the model is simply time series of the total wind farm output power $P_{\mathrm{wf}}(t)$.

The PSDs quantify the average energy in the wind speed variability, distributed on frequencies. The PSD $S_{u[i]}(f)$ of $u_{[i]}(t)$ is defined according to

$$S_{u[i]}(f) \cdot \Delta f = \left\langle U_{[i]}(f) \cdot U^{*}_{[i]}(f) \right\rangle . \tag{1}$$

$U_{[i]}(f)$ is the Fourier transform of $u_{[i]}(t)$, and Δf is the frequency step between adjacent Fourier coefficients, i.e., $\Delta f = 1/T_{\mathrm{seg}}$. The $*$ operator denotes complex conjugation, and the $\langle\rangle$ operator denotes the mean value of results from an ensemble of periods of length T_{seg}.

The simulation results are highly dependent on the specification of the wind speed PSDs. The PSDs depend on the average wind speed in the included segments, the surface roughness that generates turbulence, meteorological stability, and other external conditions. However, structural engineers use standard wind PSDs for design of buildings, bridges, and wind turbines.

For relatively high frequencies $f > 0.01$ Hz, the variability of the ambient wind speed is described by the turbulence PSDs, which are available from literature, e.g., Kaimal [13], and in codes of practice for structural engineering, e.g., the wind turbine standard IEC 61400-1 [14].

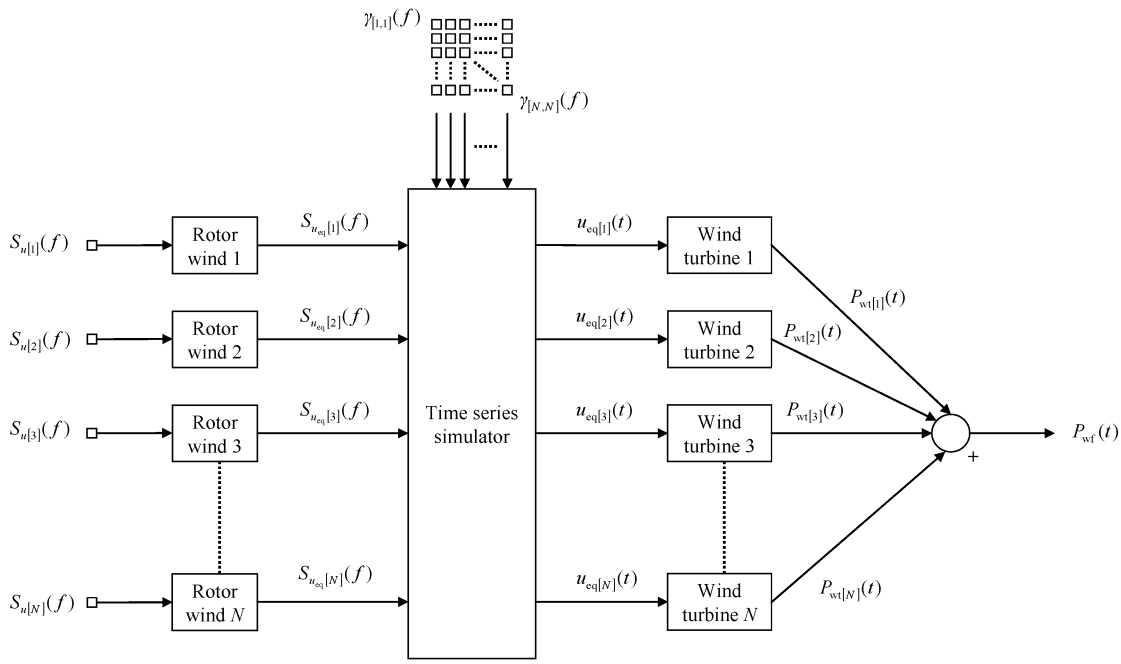

Fig. 2. Basic structure of model for simulation of power fluctuation from wind farm.

As it is seen in Fig. 2, the power fluctuation model uses individual PSDs for the individual wind turbines. This way, the added turbulence to wind speeds inside the wind farm is taken into account for the wind turbines inside the wind farm.

The added turbulence inside the wind farm is significant compared to the low ambient turbulence offshore, and for that reason, it is included in the structural design of wind turbines. The standard deviation of the added wind farm turbulence is included in the power fluctuation model, quantified according to specifications in IEC 61400-1.

The added turbulence in the wind farm is on an even shorter time scale than the ambient turbulence. The main reason why Rosas simulations [10] underestimated the power fluctuations was that the low frequency variability for frequencies $f < 0.01$ Hz was not included. There are no standards specifying the PSDs for those low frequencies. The studies of wind speed measurements from Risøs test site for large wind turbines proposed a low frequency PSD term, which is used in the present simulations.

Thus, the PSDs applied in the present model is the sum of PSDs for ambient turbulence, added wind farm turbulence, and low frequency fluctuations.

The coherence functions quantify the correlation between the wind speeds at the individual wind turbines. The definition of the coherence function $\gamma_{u[r,c]}$ between $u_{[r]}(t)$ and $u_{[c]}(t)$ is given by

$$\gamma_{u[r,c]}(f) = \frac{S_{u[r,c]}(f)}{\sqrt{S_{u[r]}(f) \cdot S_{u[c]}(f)}}. \tag{2}$$

$S_{u[r,c]}(f)$ is the cross power spectral density (CPSD) between $u_{[r]}(t)$ and $u_{[c]}(t)$, defined according to

$$S_{u[r,c]}(f) \cdot \Delta f = \left\langle U_{[r]}(f) \cdot U^*_{[c]}(f) \right\rangle. \tag{3}$$

The simulation results are also quite sensitive to the specification of the coherence functions. There are no standards specifying the horizontal coherence between wind speeds over a large distances corresponding to a wind farm. In the literature, Schlez and Infield [15] have proposed a model based on measurements in distances up to 100 m in 18-m height in Rutherford Appleton Laboratory test site, U.K., and Nanahara [16] has used measurements in distances up to 1700 m in 40-m height in Japan Sea.

There is, however, a significant difference in the conclusions of Schlez and Nanahara. In the present simulations, the results of studies in Risø National Laboratory's test site in 80-m height over 1.2-km distances are applied.

The estimation of coherence based on measurements is relatively uncertain, because coherence of wind speeds in two points strongly depends on the inflow angle, i.e., on the wind direction. Therefore, even more data are required to estimate the coherence functions than to estimate the PSDs. Thus, the assumed horizontal coherence functions are still a point with possible improvement.

The kernel of the model in Fig. 2 is the time series simulator, which converts a set of PSDs and coherence functions to a set of time series. The time series simulation can be divided into two steps. The first step is to generate a random set of Fourier coefficients fulfilling (1)–(3). When this is done, the second step is simply to apply a reverse Fourier transform to provide the time series.

The random generation of Fourier coefficients ensures that the time series simulation can generate different sets of time series, depending on a seed that initializes a random generator. The generation of Fourier coefficients ensures that an ensemble of time series generated with different seeds gets the specified PSDs and coherence functions.

A detailed mathematical description of the time series simulator is given in [9], where it is used directly on the set $S_{u[i]}(f)$ of PSDs of the hub height wind speeds. In the present model, the

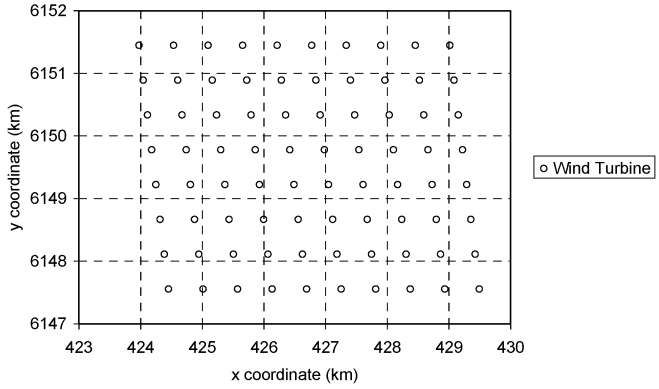

Fig. 3. Geographical layout of the Horns Rev offshore wind farm.

time series simulator is used on PSDs $S_{u\mathrm{eq}[i]}(f)$ of equivalent wind speeds $u_{\mathrm{eq}[i]}(t)$.

The equivalent wind speed $u_{\mathrm{eq}[i]}(t)$ takes into account that the wind speed is not the same over the whole wind turbine rotor. The equivalent wind speed is defined as the wind speed, which can be used in a simple aerodynamic model to calculate the aerodynamic torque on the rotor shaft as if the wind speed was equal to $u_{\mathrm{eq}[i]}(t)$ over the whole rotor. Thus, the equivalent wind speed can be obtained as a weighted average of the wind speed field in the rotor disk.

The equivalent wind speed defined in [9] includes fast periodic components that are harmonics of the rotor speed, but they are omitted in the present model because they are outside the time scale of interest for this model.

Omitting the periodic components, the equivalent wind speed $u_{\mathrm{eq}[i]}(t)$ fluctuates less than the fixed point wind speed $u_{[i]}(t)$. According to [12], the PSD of the equivalent wind speed can be found by the PSD of the fixed point wind speed, which is done by the rotor wind blocks in Fig. 2.

Finally, the wind turbine models in Fig. 2 specify the relation between the equivalent wind speed and the output power. In the present model, a simple power curve is applied, i.e., a purely steady-state model of the wind turbine. The reason for this choice is that the dynamics of the mechanical and electrical systems of the wind turbine are in a much faster time scale than the time scale of interest for the power fluctuation model.

III. Wind Farm and Data Acquisition

Horns Rev wind farm consists of 80 Vestas V80 variable speed wind turbines, using doubly-fed induction generators. The rated power of the V80 turbines is 2 MW, and the rotor diameter is 80 m.

Fig. 3 shows the layout of Horns Rev wind farm. The distance between the turbines is 560 m in the rows as well as columns, corresponding to seven rotor diameters.

The measured data are acquired by the SCADA system used by the wind farm main controller. The acquired data originate from the wind turbine control systems. For the present study, wind speeds, power, power set point, and yaw position is used.

The wind speed is measured on the nacelle of each wind turbine with ultrasonic sensors. The power is measured by the control system on the low voltage terminals as a sum of rotor and stator power. The power set point is the maximum power, which is normally 2 MW. However, the wind farm main controller sometimes lowers this value when the wind farm power limitation is active. Finally, the yaw position of the wind turbine is used to indicate the wind direction.

Data acquired from February 2005 to January 2006 are used in the present paper. Wind speed, power, and yaw position are logged with 1-Hz sampling frequency.

In some periods, the data acquisition was not working, e.g., in periods where the SCADA system had other tasks to do with higher priority. In other periods, the maximum power set point of the wind turbines was less than the normal 2 MW because the wind farm main controller was active. For the present study, data are organized in 2-h segments, where continuous data with set point 2 MW are available from minimum 70 wind turbines.

The result is 1110 segments, which corresponds to 92.5 days, i.e., significantly less than the measurement period. As mentioned above, there are many reasons for that reduction, but still a quite substantial data set is available, representing wind speeds from 1 to 19 m/s.

IV. Analyses

Parson *et al.* [7] quantified the slow variability of the wind farm power as load following and the fast as regulation, and used the one year of actual wind and load data to study the impact of the installed wind capacity on the power system in Iowa. The present study does not involve load data. Instead, ramp rates and reserve requirements are defined for the wind farm power, and duration curves are used to compare measured and simulated power fluctuations.

The definitions of ramp rates and reserve requirements are involving a statistical period time T_{per}, which reflects the time scale of interest. The time scales of interest will depend on the power system size, load behavior, and specific requirements to response times of reserves in the system. In order to study the wind variability and model performance in different time scales, the analysis of Horns Rev data is performed with 1-min, 10-min, and 30-minute period times.

For the present analysis, the measured wind farm power is calculated in p.u. as the average power of the available turbines in each 2-h segment. Thus, the reduction of the wind farm power due to non-availability of wind turbines is removed. This choice is justified because missing data from a turbine are not necessarily indicating that the turbine is not producing power but can also be because of failures in the SCADA system. Besides, the present model is not including availability, although the availability of the individual wind turbines should be added in future versions.

For each measured 2-h segment, the average wind speed and wind direction is calculated, and a 2-h wind farm power time series is simulated. The simulations are performed with the complete model including low frequency fluctuations and wind farm generated turbulence, and for comparison, simulations are also performed with ambient turbulence only. Thus, two sets of 1110 2-h time series are simulated.

A. Ramp Rates

The definition of ramp rates applied in this paper is quite similar to the definition of load following applied by Parson *et al.*

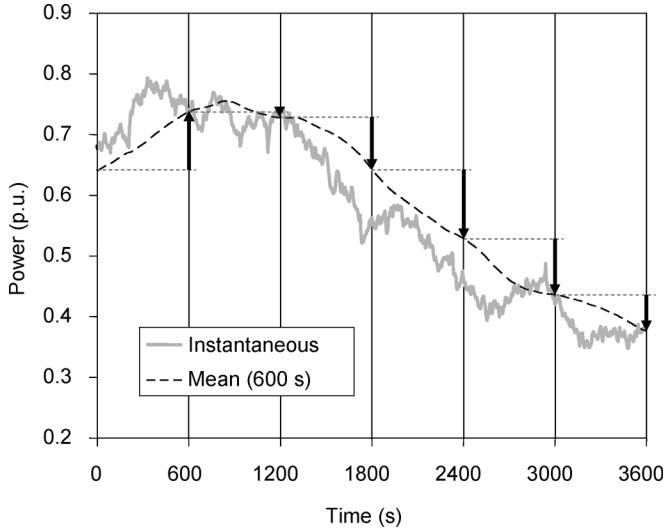

Fig. 4. Definition of ramp rated for period time $T_{\rm per} = 10$ min. The ramp rates are indicated with arrows.

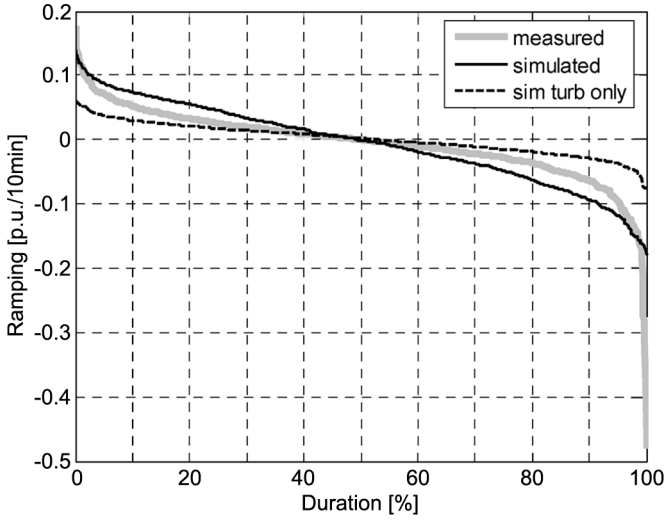

Fig. 5. Duration curves of 10-min ramp rates in the initial power range from 0.8 p.u. to 0.9 p.u.

[7]. The intention is to quantify the changes in mean values from one period $T_{\rm per}$ to another, which specifies the ramp rate requirement that the wind farm power fluctuation causes to other power plants.

The definition of ramp rates is illustrated for period time $T_{\rm per} = 600$ s in Fig. 4. The instantaneous time series of power can be either measured or simulated; in our case, both are with 1-s time steps. Then the mean value of the power is calculated at the end of each period, although it is illustrated for all time steps in Fig. 4. The ramp rate is simply the change in mean value from one period to the next, i.e.,

$$P_{\rm ramp}(n) = P_{\rm mean}(n+1) - P_{\rm mean}(n). \tag{4}$$

Note that this definition specifies the ramping of the wind farm power. Thus, negative ramp rate means decreasing wind power, which requires positive ramping of other power plants.

When the ramp rates have been calculated for each set of neighbor periods n and $n+1$ for all 1110 segments, the ramp rates are binned according to the corresponding initial power $P_{\rm mean}(n)$. This is because the statistics of the ramping will depend strongly on the initial power. For instance, the power is not likely to increase very much when it is already close to rated. A power bins of size 0.1 p.u. have been selected.

Finally, the ramping is sorted in each power bin, and a duration curve is obtained. This is done for the measurements and for the two sets of simulations. As an example, the duration curves for 10-min ramp rates in the initial power range between 0.8 p.u. and 0.9 p.u. are shown in Fig. 5.

The simulated duration curve shows higher positive and negative ramp rates than the measured duration curve, with difference less than 0.03 p.u. in most of the duration range. An exception is the last point in the measurements, which has -0.48 p.u. negative ramping.

The duration curves for the simulations with only ambient turbulence show less ramp rates than measured, which is as expected.

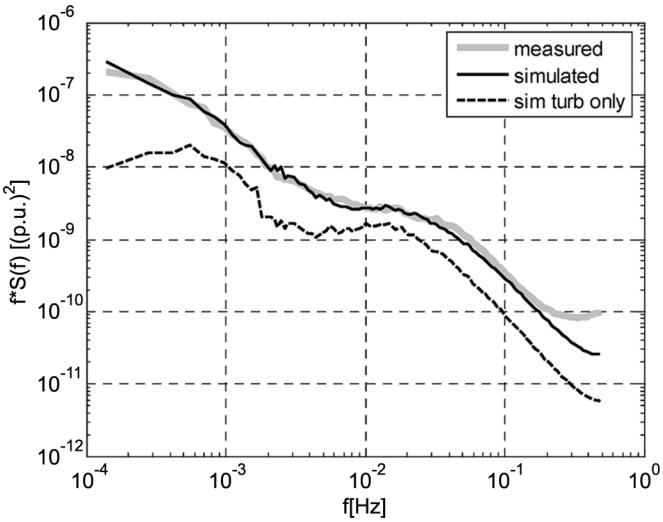

Fig. 6. PSDs of power fluctuations for 2-h segments in the power range from 0.8 p.u. to 0.9 p.u.

The PSDs of the power in the same power range are shown in Fig. 6. It is seen that there is a very good agreement between the PSDs of the measured and simulated time series, and that the PSD of the simulations with only ambient turbulence is significantly lower as expected.

The close match of the PSDs combined with the not so close match of the duration curves is not expected. Similar observations have been done for the other power ranges, although the PSDs of measured and simulated power are not matching as perfect in all power ranges.

Still, the absolute difference in the duration curves is relatively small in all power ranges, although it visually seems quite significant. The measured negative power ramp in Fig. 4 with -0.48 p.u. is also unique; similar ramps are not present in other power ranges.

A reason for the differences can be that the simulation model assumes that the Fourier coefficients at different frequencies are not correlated. In reality, some correlation is present because

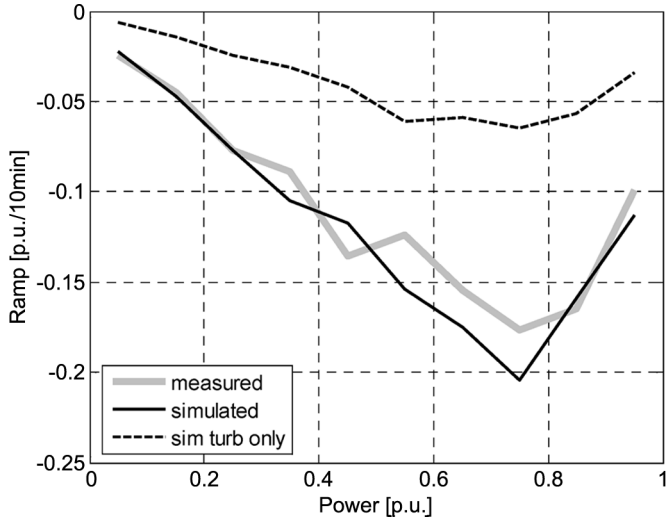

Fig. 7. The 99% percentiles of 10-min ramp rates in all power ranges.

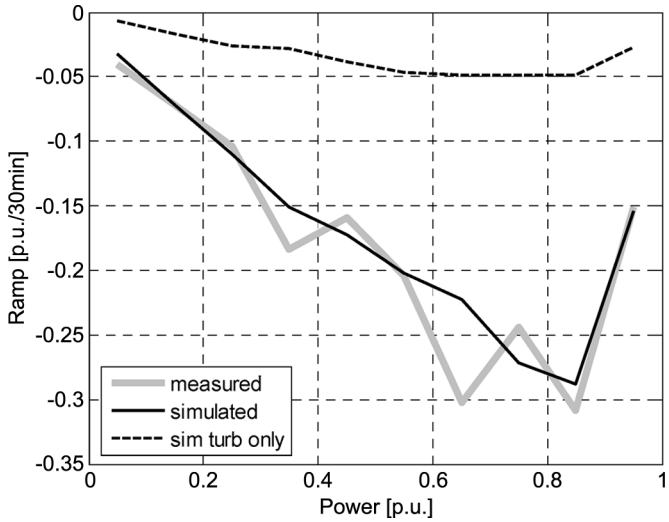

Fig. 8. The 99% percentiles of 30-min ramp rates in all power ranges.

the general level of turbulence and low frequency fluctuations depend on the weather conditions in the individual 2-h segment. Such a correlation is relatively easy to include formally in the model, but further studies of the meteorology are required to quantify the correlation properly.

Still, the most interesting point of the duration curves is around 100%, where the highest requirement to the ramp rates of other power plants is quantified. The wind farm positive ramp rates can be limited directly by the ramp limiter in wind farm main controller.

For that reason, the 99% percentile of the duration curves for 10-min ramp rates are shown for all power range bins in Fig. 7. Generally, the match between the measured and simulated curve is very good, with differences less than 0.03 p.u./10 min. Also, it is confirmed that the simulation with ambient turbulence underestimates the ramp rates significantly in all power ranges.

The 99% percentiles are shown for 30-min period times in Fig. 8. Also here, the agreement is very good, with less than 0.03 p.u./30 min difference between measured and simulated ramp rates.

Finally, the ramp rates are shown with 1-min period time in Fig. 9. Although the difference between measured and simulated looks significant, it is less than 0.015 p.u./1 min.

Summarizing the ramping analysis, the 99% percentiles of the simulated series agree quite well with the measured time series. Another observation is that the ramping shows a tendency to increase until 0.9 p.u. and then decrease a little in the last power bin. This is because the wind farm ramps less for wind speeds above rated, where the wind turbines are working on the flat part of the power curve.

B. Reserve Requirements

The definition of reserve requirements applied in this paper is quite similar to the definition of regulation applied by Parson *et al.* [7]. The intention is to quantify the difference between the instantaneous power and the mean value that are dealt with as ramping. Since the reserves must be allocated in advance, the positive reserve requirement is defined as the difference between the initial mean value and the minimum value in the next period.

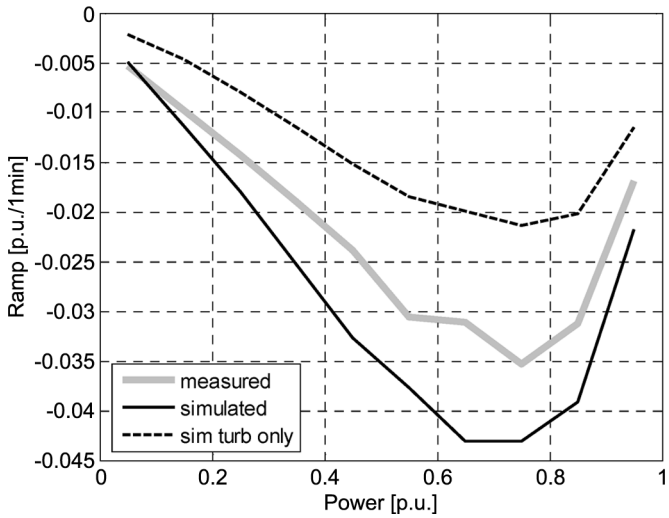

Fig. 9. The 99% percentiles of 1-min ramp rates in all power ranges.

This definition of reserve requirements is illustrated for period time $T_{\mathrm{per}} = 600\,\mathrm{s}$ in Fig. 10. Formally, the reserve requirements are defined as

$$P_{\mathrm{res}}(n) = P_{\mathrm{mean}}(n) - P_{\mathrm{min}}(n+1). \tag{5}$$

Note that with this definition, positive reserves mean decreasing wind power that requires positive reserves from other power plants.

The duration curves are then calculated for the reserves in all power bins, and the 1% percentiles are found in each power bin.

The resulting 1% percentiles with 10-min, 30-min, and 1-min period times are shown in Figs. 11–13, respectively.

It is concluded that the simulated time series agree quite well with those measured in the prediction of reserves. Also the reserve requirement decreases in the highest power bin because the wind speed is above rated.

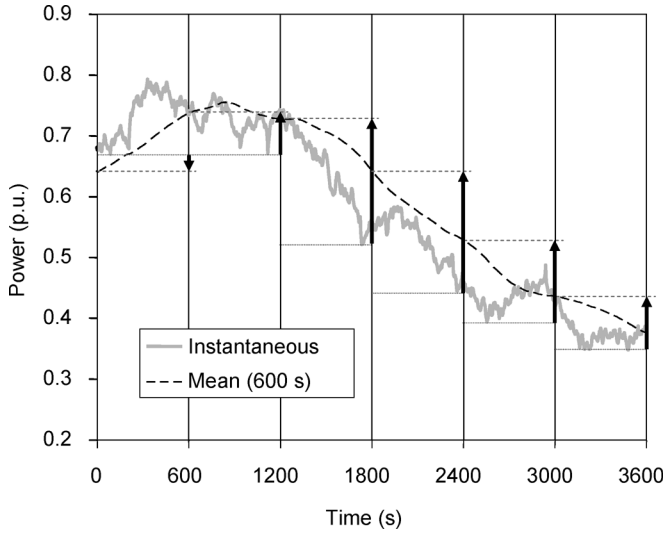

Fig. 10. Definition of reserve requirements for period time $\mathrm{Tper} = 10\ \mathrm{min}$. The reserves are indicated with arrows.

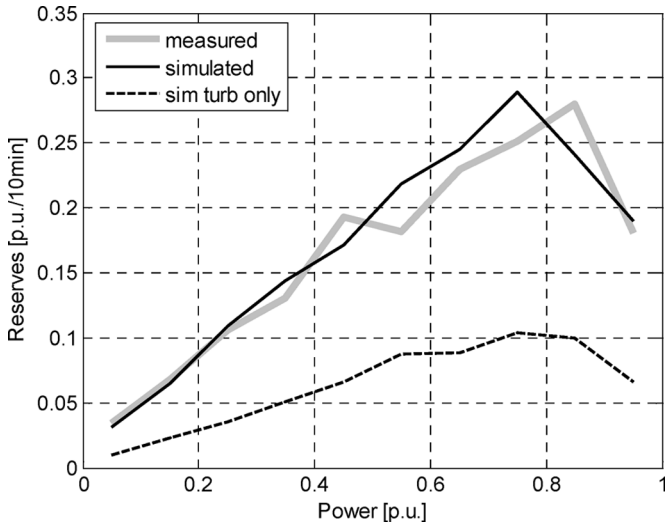

Fig. 11. The 1% percentiles of 10-min reserve requirements.

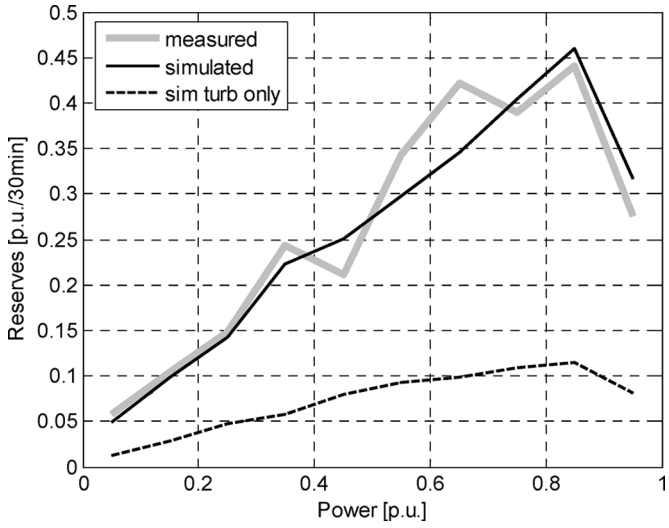

Fig. 12. The 1% percentiles of 30-min reserve requirements.

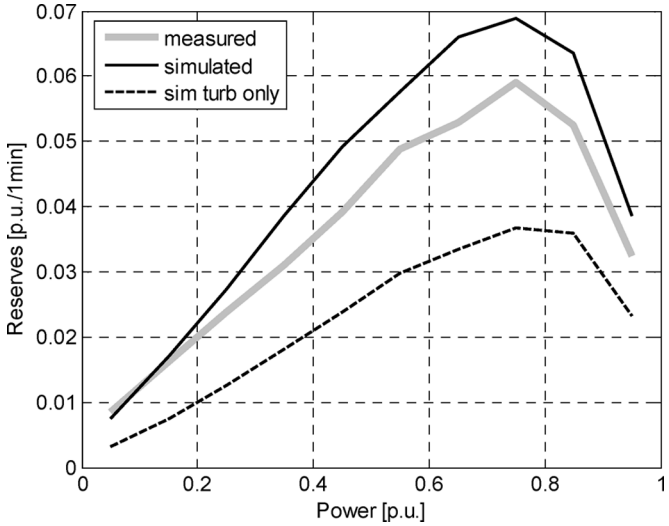

Fig. 13. The 1% percentiles of 1-min reserve requirements.

V. Conclusion

The conclusion is that the development of wind power in some power systems has reached a level where the fluctuations from wind farms play an increasing role on the need for ramping and reserve capacities in the systems.

The wind power fluctuations influence the area control in interconnected systems and the frequency control and system security in smaller island systems.

Large wind farms contribute with more power fluctuation to the system than a similar capacity of distributed wind power. This is because a large wind farm is concentrated in a geographically small area, where the slow wind fluctuations at the wind turbines are much correlated, while the correlation over longer distances is much smaller.

The extreme percentiles in the duration curves indicate that the ramp rate is up to 0.25 p.u./10 min, and the 10-min reserve requirement to other power plants is 0.35 p.u. when the wind farm is producing 0.8–0.9 p.u.

The simulation model predicts the PSDs of the power simulations very well. Duration curves for ramp rates and reserve requirements are generally simulated to slightly higher values than measured, but the extreme values obtained from simulations agree very well with those measured.

It is very important for the simulation model to include the slow variations in wind speeds that are not represented by standard turbulence PSDs.

References

[1] B. M. Weedy and B. J. Cory, *Electric Power Systems*, 4th ed. Chichester, U.K.: Wiley, 1998, ch. 4.
[2] [Online]. Available: http://www.nordpool.com.
[3] Nordic Grid Code: Nordel, Jun. 2004.
[4] I. Troen and L. Landberg, "Short term prediction of local wind conditions," in *Proc. Eur. Community Wind Energy Conf.*, Madrid, Spain, 1990, pp. 76–78.
[5] V. Akhmatov, H. Abildgaard, J. Pedersen, and P. B. Eriksen, "Integration of offshore wind power into the western danish power system," in *Proc. Offshore Wind*, Copenhagen, Denmark, 2005.
[6] J. R. Kristoffersen, "The Horns Rev wind farm and the operational experience with the wind farm main controller," in *Proc. Offshore Wind*, Copenhagen, Denmark, 2005.

[7] B. Parson, M. Milligan, B. Zavadil, D. Brooks, B. Kirby, K. Dragoon, and J. Caldwell, "Grid impacts of wind power: A summary of recent studies in the united states," *Wind Energy*, vol. 7, pp. 87–108, Apr./Jun. 2004.
[8] D. Brooks, J. Smith, E. Lo, S. Ishikawa, L. Dangelmaier, and M. Bradley, "Development of a methodology for the assessment of system operation impacts of integrating wind generation on a small island power system," in *Proc. Eur. Wind Energy Conf.*, London, U.K., 2004.
[9] P. Sørensen, A. D. Hansen, and P. A. C. Rosas, "Wind models for simulation of power fluctuations from wind farms," *J. Wind Eng. Ind. Aerodynam.*, vol. 90, pp. 1381–1402, Dec. 2002.
[10] P. A. C. Rosas, "Dynamic influence of wind power on the power system," Ph.D. dissertation, Tech. Univ. Denmark, Lyngby, Denmark, Risø-R-1408.
[11] P. Sørensen, J. Mann, and U. S. Paulsen, "Large scales wind speeds," in *Abstracts EGU General Assembly*, Vienna, Austria, April 2006.
[12] P. Sørensen, N. A. Cutululis, A. Vigueras-Rodríguez, H. Madsen, P. Pinson, L. E. Jensen, J. Hjerrild, and M. Donovan, "Modelling of power fluctuations from large offshore wind farms," *Wind Energy*, invited paper submitted for publication for special issue .
[13] J. C. Kaimal, J. C. Wyngaard, Y. Izumi, and O. R. Cote, "Spectral characteristics of surface-layer turbulence," *Q. J. R. Meteorol. Soc.*, vol. 98, pp. 563–598, 1972.
[14] *Wind Turbines—Part 1: Design Requirements*, Int. Std. IEC 61400-1, 3rd Ed. 2005-2008.
[15] W. Schlez and D. Infield, "Horizontal, two point coherence for separations greater than the measurement height," *Boundary-Layer Meteorol.*, vol. 87, pp. 459–480, 1998.
[16] T. Nanahara, M. Asari, T. Sato, K. Yamaguchi, M. Shibata, and T. Maejima, "Smoothing effects of distributed wind turbines. Part 1. Coherence and smoothing effects at a wind farm," *Wind Energy*, vol. 7, pp. 61–74, Apr./Jun. 2004.

Poul Sørensen (M'04–SM'07) was born in 1958. He received the M.Sc. degree in electrical engineering from the Technical University of Denmark, Lyngby, in 1987.

Since 1987, he has been employed at Risø National Laboratory, Roskilde, Denmark, presently as a Senior Scientist. His main technical interest is integration of wind power into power systems, involving a variety of technical disciplines including power system control and stability, dynamic modeling and control of wind turbines and wind farms, and wind fluctuation statistics.

Nicolaos Antonio Cutululis (M'07) was born in 1974. He received the M.Sc. and Ph.D. degrees in electrical engineering from the "Dunarea de Jos" University of Galati, Galati, Romania, in 1998 and 2005, respectively.

Since February 2005, he has been employed at Risø National Laboratory, Roskilde, Denmark, as a Postdoctoral fellow. His main interest is wind power systems dynamic modeling, simulation, and control.

Antonio Vigueras-Rodríguez was born in 1980.

He became an industrial engineer in the Technical University of Cartagena (UPCT), Cartagen, Spain, in 2003. He is employed at UPCT in a Ph.D. position (supported by the Spanish program of FPU grants), related with modeling of wind turbines, wind farms and wind fluctuations.

Leo E. Jensen received the M.Sc. degree in mechanical engineering from Aalborg University, Aalborg, Denmark, in 1989.

Since then, he has dedicated his efforts to wind power engineering and has achieved an overall in-depth knowledge of this field. In addition to training experience, his major fields of expertise comprise wind energy resource calculations, aerodynamic calculations, structural analysis including fatigue life investigation and codes, certification criteria, and procedures.

Mr. Jensen is an appointed member of the committee of experts on wind turbine certification at Det Norske Veritas (DNV), Denmark, and the advisory board on the turbine certification scheme of the Danish Energy Authority.

Jesper Hjerrild was born in 1971. He received the M.Sc. and Ph.D. degrees in electrical engineering from the Technical University of Denmark, Lyngby, in 1999 and 2002, respectively.

He was employed at DEFU (The Association of Danish Energy Companies, R&D) from 2002 until 2004. Since 2004, he has been employed at Elsam (now a part of Dong Energy). His main technical interest is electrical power systems in general, involving a variety of technical disciplines including modeling of power system including wind power and power system control and stability. Furthermore, he also works with designing of the wind farm.

Martin Heyman Donovan was born in 1971. He received the M.Sc. degree in energy engineering from the Technical University of Denmark, Lyngby, in 1998.

He was employed at SEAS from 2000–2003 and is presently employed at Energy E2 as project leader for the SCADA system for Horns Rev. His main interests are SCADA and automation systems for wind farms. He has been one of the designers of the power control systems for Nysted Offshore Windfarm.

Henrik Madsen received the M.Sc. degree in engineering and the Ph.D. in statistics from the Technical University of Denmark (DTU), Lyngby, in 1982 and 1986, respectively.

He was appointed Assistant Professor in statistics in 1986, Associate Professor in 1989, and Professor in statistics with a special focus on stochastic dynamic systems in 1999. He has been an external lecturer at a number of universities. His main research interest is related to analysis and modeling of stochastic dynamics systems. He has authored or coauthored approximately 280 papers and technical reports and about ten educational texts. He is the leader of "Center for High Performance Computing" at DTU, which was opened by the Danish Minister of Research in February 2002.